

## Article

# Effects of Phosphorus and Boron Compounds on Thermal Stability and Flame Retardancy Properties of Epoxy Composites

Corneliu Hamciuc <sup>1</sup>, Tăchiță Vlad-Bubulac <sup>1,\*</sup>, Diana Serbezeanu <sup>1</sup>, Ana-Maria Măcsim <sup>1</sup>, Gabriela Lisa <sup>2</sup>, Ion Anghel <sup>3</sup> and Ioana-Emilia Șofran <sup>3</sup>

<sup>1</sup> Department of Polycondensation and Thermally Stable Polymers, “Petru Poni” Institute of Macromolecular Chemistry, 41A, Grigore Ghica Voda Alley, 700487 Iasi, Romania

<sup>2</sup> Department of Chemical Engineering, Gheorghe Asachi Technical University of Iasi, Faculty of Chemical Engineering and Environmental Protection, Bd. Mangeron 73, 700050 Iasi, Romania

<sup>3</sup> Police Academy “Alexandru Ioan Cuza”, Fire Officers Faculty, Morarilor Str. 3, Sector 2, 022451 Bucharest, Romania

\* Correspondence: tvlabdb@icmpp.ro

**Abstract:** While plastics are regarded as the most resourceful materials nowadays, ranging from countless utilities including protective or decorating coatings, to adhesives, packaging materials, electronic components, paintings, furniture, insulating composites, foams, building blocks and so on, their critical limitation is their advanced flammability, which in fire incidents can result in dramatic human fatalities and irreversible environmental damage. Herein, epoxy-based composites with improved flame-resistant characteristics have been prepared by incorporating two flame retardant additives into epoxy resin, namely 6-(hydroxy(phenyl)methyl)-6H-dibenzo[*c,e*][1,2]oxaphosphinine-6-oxide (PFR) and boric acid ( $H_3BO_3$ ). The additional reaction of 9,10-dihydro-oxa-10-phosphophenanthrene-10-oxide (DOPO) to the carbonyl group of benzaldehyde yielded PFR, which was then used to prepare epoxy composites having a phosphorus content ranging from 1.5 to 4 wt%, while the boron content was 2 wt%. The structure, morphology, thermal stability and flammability of resulted epoxy composites were investigated by FTIR spectroscopy, scanning electron microscopy (SEM), thermogravimetric analysis, differential scanning calorimetry, and microscale combustion calorimetry (MCC). Thermogravimetric analysis indicated that the simultaneous incorporation of PFR and  $H_3BO_3$  improved the thermal stability of the char residue at high temperatures. The surface morphology of the char residues, studied by SEM measurements, showed improved characteristics in the case of the samples containing both phosphorus and boron atoms. The MCC tests revealed a significant reduction in flammability as well as a significant decrease in heat release capacity for samples containing both PFR and  $H_3BO_3$  compared to the neat epoxy thermoset.

**Keywords:** epoxy composites; phosphorus-containing flame retardant; boric acid; thermal stability; flame resistant



**Citation:** Hamciuc, C.; Vlad-Bubulac, T.; Serbezeanu, D.; Măcsim, A.-M.; Lisa, G.; Anghel, I.; Șofran, I.-E. Effects of Phosphorus and Boron Compounds on Thermal Stability and Flame Retardancy Properties of Epoxy Composites. *Polymers* **2022**, *14*, 4005. <https://doi.org/10.3390/polym14194005>

Academic Editors: Marcos Batistella and Laurent Ferry

Received: 31 August 2022

Accepted: 20 September 2022

Published: 24 September 2022

**Publisher’s Note:** MDPI stays neutral with regard to jurisdictional claims in published maps and institutional affiliations.



**Copyright:** © 2022 by the authors. Licensee MDPI, Basel, Switzerland. This article is an open access article distributed under the terms and conditions of the Creative Commons Attribution (CC BY) license (<https://creativecommons.org/licenses/by/4.0/>).

## 1. Introduction

Epoxy resins represent one of the most developed classes of thermosetting polymers due to their numerous applications in the construction, transportation, aerospace industry, biomedical systems, electrical and electronic fields. They have excellent mechanical properties, good thermal and chemical resistance, good electrical insulating properties, and low shrinkage after curing [1–3]. Epoxy resins have been widely used as polymeric matrices for the preparation of composites with improved characteristics. The properties of composites depend on the structure of the resins, curing agent, and organic or inorganic fillers [4–6]. However, cured epoxy resins have high flammability, which reduces their application in areas where flame-resistant polymeric materials are required. A commonly used method to improve their flame resistance characteristics is to incorporate flame retardant additives into epoxy resins [7–9]. In the last decades, conventional halogenated flame retardants

have been frequently mixed with epoxy resins to improve their flame resistance, but these compounds can release toxic chemicals into the environment and by combustion can produce very dangerous toxic compounds [10,11]. Therefore, much research has been done to develop new environmentally friendly high-efficiency flame retardant additives.

Phosphorus-containing flame retardants have received extensive attention because they are environmentally friendly, highly efficient in reducing the flammability of polymers, and do not produce very toxic compounds by burning [12–18]. A special class of phosphorus-containing flame retardants frequently used to improve the flame-resistant properties of epoxy resins is represented by 9,10-dihydro-9-oxa-10-phosphaphenanthrene-10-oxide (DOPO) and their derived compounds [19–21]. It has been demonstrated in numerous studies that due their high degree of aromaticity they exhibit high flame retardant performance. These flame retardants present a twofold mechanism of flame inhibition: on one hand in the gas phase by producing PO· radicals, and on the other hand in the solid phase by their direct interaction with the decomposition species evolved from the polymer backbone, to produce a more compact carbonaceous char layer on the surface of the polymeric material [8,20–26].

A literature survey reveals that boron-containing compounds can be also used as flame retardant additives for epoxy resins [27,28]. These compounds improve the flame resistance of the polymers by acting in the gas and the condensed phases. They decompose endothermically, reducing the temperature of the system and producing water that can dilute flammable gases that result from the pyrolysis process [29]. In the condensed phase, they improve the formation and stabilization of a protective char layer on the polymer surface [30,31]. The presence of inorganic particles in the epoxy resin may provide useful characteristics such as heat resistance and flame retardancy. The incorporation of boric acid ( $H_3BO_3$ ) particles into epoxy resin leads to a significant modification of the structure and properties of epoxy thermosets, and to a reduction in the flammability of the composites.  $H_3BO_3$  is colorless, inexpensive, and exhibits low volatility and relatively low toxicity. This compound eliminates water at a temperature higher than 100 °C [32,33]. The water released during its decomposition reduces the temperature and can dilute the combustible gases in the combustion zone. At higher temperatures,  $H_3BO_3$  is converted to boric trioxide ( $B_2O_3$ ) [34,35] which can form a glassy film on the burning surface of the polymer, thus inhibiting the diffusion of flammable gases in the combustion zone and reducing the flame spread on the polymer surface [36,37].

One way to increase the effectiveness of flame retardants and to reduce the costs associated with their use is to incorporate into epoxy resins two flame retardants that have a synergistic effect in reducing flammability. Several studies have demonstrated that boron-containing flame retardants have a synergistic effect with flame retardants containing phosphorus and nitrogen atoms in improving the flame retardancy of epoxy resins [28]. They improve the char formation with efficient barrier properties and promote the increase in the phosphorus content in the condensed phase [38,39].

In this study, a phosphorus-containing DOPO derivative (PFR) and  $H_3BO_3$  were introduced into epoxy resin to improve its flame resistance. The main advantage of choosing PFR and  $H_3BO_3$ , over other phosphorus-containing flame retardants with complicated architectures that require difficult and time-consuming preparation methods, is related to the simple and cost-effective synthetic procedure of PFR and the ready commercial availability of boric acid, which is doubled by the expected synergistic effect of the two flame retardants. The effect of  $H_3BO_3$  and PFR containing phosphorus on decreasing the flammability of epoxy resin was studied. Scanning electron microscopy was used to investigate the morphology of the cured epoxy composites and the char layer resulting from the pyrolysis of the samples. The thermal stability and flame retardance of the composites were investigated by thermogravimetric analysis and microscale combustion calorimetry tests.

## 2. Materials and Methods

### 2.1. Materials

The 9,10-Dihydro-oxa-10-phosphophenanthrene-10-oxide (DOPO, 14.32% P) was purchased from Chemos GmbH (Germany) and was freshly dehydrated before use. Benzaldehyde and  $H_3BO_3$  (17.48% B, having the mean particle size distribution of 74.395  $\mu m$ ) were supplied by Sigma-Aldrich and used as received. The two-component based epoxy resin used as the polymeric matrix was supplied by DEVE PRODEXIM Oradea, Romania. The first component (EP) consists in a mixture of bisphenol A diglycidyl ether and an adduct of oxirane with mono (C12-C14-alkoxy) methyl derivatives. The second component (HA), used as a hardener, is a mixture of benzyl alcohol, 3-aminomethyl-3,5,5-trimethylcyclohexylamine, m-phenylenebis(methylamine) and bisphenol-A.

### 2.2. Synthesis of 6-(Hydroxy(phenyl)methyl)-6H-dibenzo[c,e][1,2]oxaphosphinine-6-oxide

The 6-(Hydroxy(phenyl)methyl)-6H-dibenzo[c,e][1,2]oxaphosphinine-6-oxide (PFR) was prepared by the additional reaction of the P-H group of DOPO to the carbonyl group of benzaldehyde, as was previously described in the literature [40]. Benzaldehyde (10.6 g, 0.1 mol), DOPO (23.76 g, 0.11 mol) and toluene (190 mL) were placed in a 500 mL three-necked glass flask equipped with a magnetic stirrer, temperature regulator, and reflux condenser. The reaction mixture was heated at 110 °C for 10 h under a nitrogen atmosphere. After the reaction was complete, the mixture was cooled to ambient temperature and the resulting precipitate was filtered off. The product was dried in a vacuum oven at 60 °C for 4 h.

Yield: 93%. (30.97% P).

FTIR (KBr,  $cm^{-1}$ ): 935 (P–O–Ph stretching vibrations), 1203 (P=O stretching vibrations), 1474 (P–Ph aromatic ring in-plane stretching vibrations), 3245 (O–H stretching vibrations).  $^1H$  NMR ( $CDCl_3-d_1$ ): 3.15 (1 H, bs, OH one isomer), 3.58 (1 H, bs, OH second isomer), 5.26 (1 H, d, JH-P = 6.9 Hz, H-5 one isomer), 5.31 (1 H, d, JH-P = 9.4 Hz, H-5-s isomer), 7.19–7.08 (8 H, m, H-1 both isomers, H-2 both isomers, H-14 both isomers, H-16 both isomers), 7.33–7.23 (7 H, m, H-15 both isomers, H-3 both isomers), 7.47–7.40 (2 H, m, H-9 both isomers), 7.72–7.63 (3.5 H, m, H-8 both isomers, H-10 one isomer, H-13 one isomer), 7.97–7.81 (4 H, m, H-7 both isomers, H-10 s isomer, H-13 s isomer).

$^{13}C$  NMR ( $CDCl_3-d_1$ ): 73.55 (d, JC-P = 113.1 Hz, C-5 one isomer), 73.73 (d, JC-P = 109.6 Hz, C-5 s isomers), 119.93–119.86 (C-16 both isomers), 121.82–121.10 (m, C-11 both isomers, C-12 both isomers), 122.9 (d, JC-P = 11.1 Hz, C-7 one isomer), 123.3 (d, JC-P = 10.0 Hz, C-7 s isomer), 124.2 (d, JC-P = 7.0 Hz, C-14 both isomers), 124.8 (d, JC-P = 11.8 Hz, C-13 both isomers), 127.02–126.97 (m, C-3 both isomers), 128.31–127.91 (m, C-9 both isomers, C-1 both isomers, C-2 both isomers), 130.4 (d, JC-P = 8.3 Hz, C-15 both isomers), 132.10–131.88 (m, C-10 both isomers), 133.7 (d, JC-P = 10.2 Hz, C-8 both isomers), 134.9 (d, JC-P = 15.9 Hz, C-4 both isomers), 136.92–136.79 (m, C-6 both isomers), 150.35–150.18 (m, C-17 both isomers).

### 2.3. Preparation of Epoxy Resin Composites

Various amounts of PFR were mixed with Epoxy, under stirring at 130 °C for 30 min. The mixtures were cooled to 50 °C, and  $H_3BO_3$  was introduced. They were ultrasonicated for 30 min and cooled to 25 °C. Then HA hardener was added, and the stirring was continued for 30 min. The product was cured at room temperature for 24 h, and at 60 °C for 4 h. The formulation of the epoxy resin, PFR and  $H_3BO_3$  pre-curing mixtures is listed in Table 1.

**Table 1.** Preparation details of epoxy resin composites.

Sample	Epoxy Resin (EP) (g)	Hardener (HA) (g)	Flame Retardant (PFR) (g)/(%)	H <sub>3</sub> BO <sub>3</sub> (g)/(%)	Phosphorus (wt%)	Boron (wt%)
EP-0	10	5	-	-	0	0
EP-1	3.96	1.98	1.56/0.12	-	2	0
EP-2	2.35	1.17	1.58/0.08	-	3	0
EP-3	2.92	1.46	3.14/0.23	-	4	0
EP-4	2.48	1.24	0.73/0.04	0.42/0.02	1.5	2
EP-5	3.39	1.70	1.55/0.12	0.86/0.06	2	2

#### 2.4. Measurements

The structure of PFR was investigated by using FTIR and NMR spectroscopy. The FTIR spectrum was recorded on a FTIR Bruker Vertex 70 Spectrophotometer. The proton and carbon NMR experiments were recorded on Bruker Avance NEO 400 MHz operating at 400.1 and 100.6 MHz, equipped with a 5 mm direct detection four nuclei probe (H, C, Si, F). The phosphorus NMR spectrum was recorded on a Bruker Avance NEO 600 MHz operating at 600.1 MHz and 242.9 MHz, equipped with a 5 mm inverse detection multinuclear probe. <sup>1</sup>H and <sup>13</sup>C NMR chemical shifts ( $\delta$ ) in ppm are calibrated to residual solvent peaks (CDCl<sub>3</sub>, 7.26 ppm for <sup>1</sup>H and 77.01 ppm for <sup>13</sup>C).

The structure of the thermosets was determined by FTIR spectroscopy using a BioRad 'FTS 135' FTIR spectrometer equipped with a Specac "Golden Gate" ATR accessory. A LUMOS Microscope Fourier Transform Infrared (FTIR) spectrophotometer (Bruker Optik GmbH, Ettlingen, Germany), equipped with an attenuated total reflection (ATR) device, was used to record the scans between 4000 and 600 cm<sup>-1</sup> at a resolution of 4 cm<sup>-1</sup>.

Microscopic investigations of epoxy thermosets and of their corresponding chars were performed on an Environmental Scanning Electron Microscope Type Quanta 200, operating at 10 kV with secondary electrons in a low vacuum mode (LFD detector). The Quanta 200 microscope is equipped with an Energy Dispersive X-Ray (EDX) system for qualitative and quantitative analysis and elemental mapping.

Thermogravimetric (TG) curves and thermogravimetric derivative (DTG) curves of PFR and epoxy thermosets were recorded with Mettler Toledo TGA-SDTA851e equipment, in a nitrogen atmosphere, and a heating rate of 10 °C min<sup>-1</sup>, in the temperature range of 25–800 °C. Differential scanning calorimetry (DSC) measurements of PFR and epoxy thermosets were carried out using a Mettler Toledo DSC1 type device in an inert atmosphere, with a heating rate of 10 °C min<sup>-1</sup> and nitrogen purge at 100 mL min<sup>-1</sup>.

The flammability behavior of PFR and epoxy thermosets was tested using an FTT Micro Calorimeter [41].

### 3. Results and Discussion

#### 3.1. Synthesis and Characterization of PFR

PFR was prepared by adding DOPO monomer to the carbonyl group of benzaldehyde, following an adapted method previously reported [40]. The reaction took place in toluene, at 110 °C for 10 h. The structure of PFR was characterized by FTIR, <sup>1</sup>H NMR, <sup>13</sup>C NMR and <sup>31</sup>P NMR spectroscopy. The NMR analysis of PFR showed the existence of two diastereomers in molar ratio of 1:0.7. This phenomenon has been reported in the literature [42] and it was attributed to the chirality of the phosphorus stereocenter of DOPO. The presence of the phosphorus atom in the structure complicates the shape of the signals in the NMR spectra. The <sup>1</sup>H NMR spectrum of PFR displays some characteristic signals: the hydroxyl group has a broad resonance signal in the region 3.15–3.58 ppm, the CH group proton was associated with the two doublets (one for each isomer) from 5.31 ppm and 5.26 ppm, and all aromatic protons have complex resonance signals were in the region 7.00–8.00 ppm,

mainly due to the proton–phosphorus couplings, and also due to the presence of the two isomers causing more overlap of the signals (Figure 1).

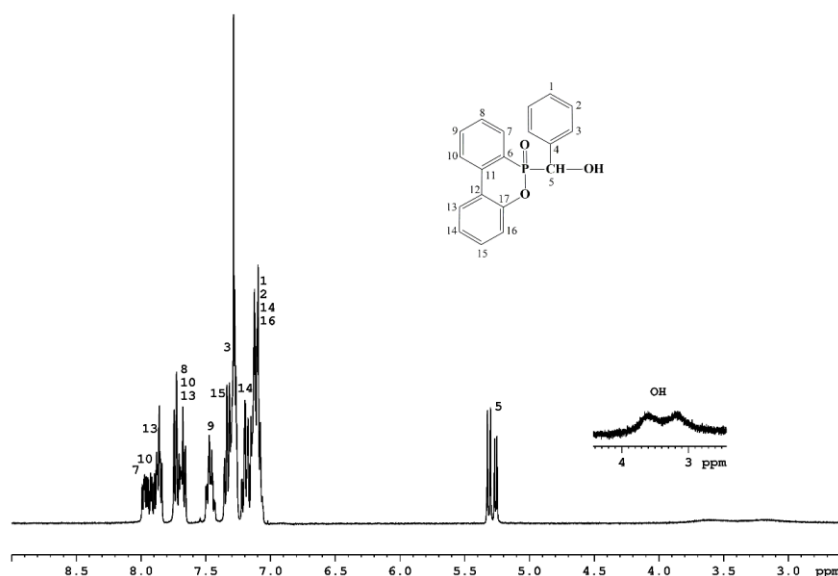


Figure 1.  $^1\text{H}$  NMR spectrum of PFR.

In the case of the carbon spectrum, all the signals appear as doublets or multiplets due to carbon–phosphorus coupling. As can be seen in Figure 2, the CH group has two characteristic doublets at 73.5 ppm and 73.7 ppm while the signals for the aromatic carbon atoms appear in the range 118 ppm to 151 ppm, the quaternary carbon directly linked to oxygen being the most de-shielded in the interval 150.1–150.3 ppm. The existence of the two isomers is clearly seen in the  $^{31}\text{P}$  NMR spectra, by the presence of two signals at 31.88 ppm and 30.65 ppm, respectively (Figure 2 inset).

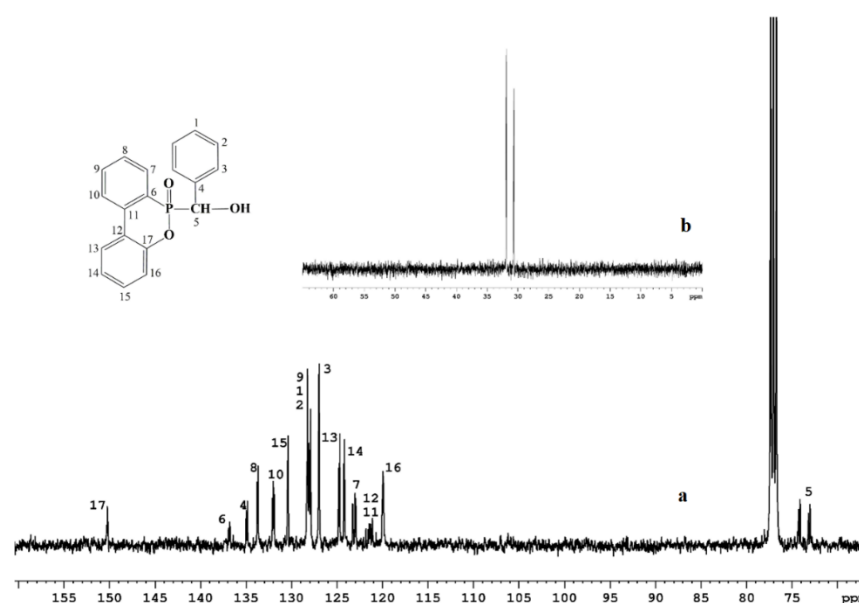


Figure 2.  $^{13}\text{C}$  NMR (a) and  $^{31}\text{P}$  NMR (b) spectra of PFR.

The thermal properties of PFR were investigated by TGA analysis. The TG and DTG curves of PFR showed that it decomposed in two steps (Figure 3). The first decomposition step was in the temperature range of 180–320 °C, which may be attributed to the catalysis of acidic phosphorus-based products evolved during the thermal decomposition

of oxaphosphinine-6-oxide structure, while the second step took place in the interval of 320–520 °C as a result of the further thermal decomposition of the enriched aromatic carbonaceous structure [43]. The maximum weight loss rate in the first step of decomposition was 0.55 %/°C while the maximum weight loss rate of the second step of decomposition was lower (0.34 %/°C). The temperature at which the mass loss rate is the highest in the thermal decomposition process of the first step of decomposition was 208 °C, while that of the second step of decomposition appeared at 408 °C.

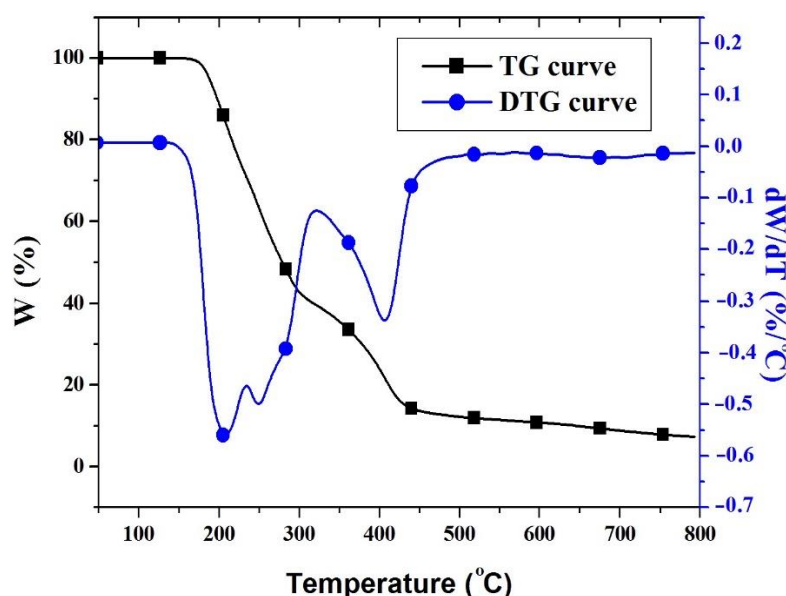


Figure 3. TG and DTG curves of PFR.

### 3.2. Structural and Morphological Characterization of Epoxy-Based Composites

Epoxy-based composites were prepared by incorporation of PFR and  $H_3BO_3$  in epoxy resin (Figure 4). The PFR content was adjusted so that the phosphorus atom concentration varies between 0 and 4 wt%.  $H_3BO_3$  content was calculated to have a concentration of 2 wt% of boron in the thermosets (Table 1).

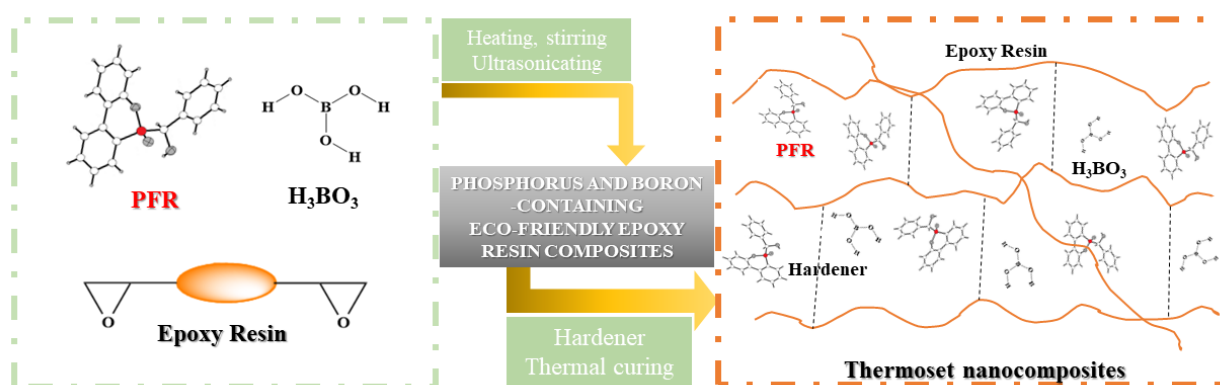


Figure 4. Graphical representation of epoxy composites synthetic pathway.

The resulting thermoset structures were investigated by FTIR spectroscopy (Figure 5). The neat EP-0 system presented characteristic absorption bands at  $3350\text{ cm}^{-1}$  (O-H stretching vibrations),  $3053\text{ cm}^{-1}$  (C-H tension of the methylene group of the epoxy ring (stretching vibrations)),  $2926$  (aliphatic C-H asymmetric stretching vibrations),  $2865\text{ cm}^{-1}$  (aliphatic C-H symmetric stretching vibrations),  $1610$  and  $1510\text{ cm}^{-1}$  (aromatic C=C stretching vibration),  $1240$  and  $1036\text{ cm}^{-1}$  (aromatic ether C-O-C asymmetric and symmetric stretching vibrations, respectively). The EP containing phosphorus and boron additives (EP1-EP5)

exhibited characteristic absorption peaks at 3340 (O–H and N–H stretching vibrations), 2960 and 2865  $\text{cm}^{-1}$  (aliphatic C–H stretching vibrations), 1607 and 1510  $\text{cm}^{-1}$  (aromatic C=C stretching vibrations), 933  $\text{cm}^{-1}$  (aromatic P–O–C stretching vibrations), 754  $\text{cm}^{-1}$  (deformation vibrations caused by the 1,2-disubstituted aromatic phosphaphenanthrene rings) and 699  $\text{cm}^{-1}$  (deformation vibrations of the aromatic rings).

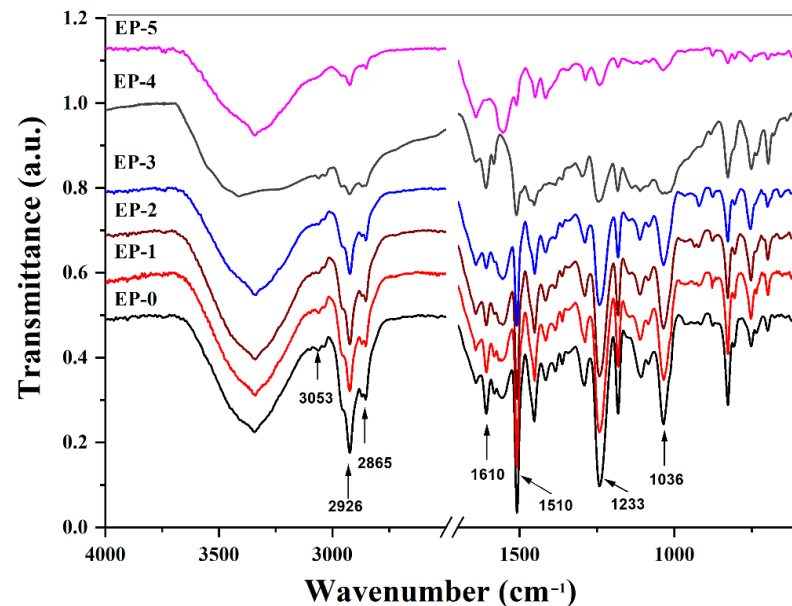


Figure 5. FTIR spectra of EP epoxy composites.

Scanning electron microscopy (SEM) characterization was used to investigate the morphology in the fracture surfaces of cured epoxy resin and its composites. Certain amounts of each sample were immersed under liquid nitrogen, then they were broken by applying mechanical stress. The SEM micrographs taken upon the fractured area of each sample are shown in Figure 6. The neat epoxy resin EP-0 had a smooth fracture surface, and showed a typical brittle fracture. When PFR was incorporated into epoxy resin, different rough fracture surfaces were observed (EP-1, EP-2 and EP-3). The maximum in fracture roughness increased with the amount of PFR content. In the case of EP-4 and EP-5 containing 2 wt% boron and 1.5 and 2 wt% phosphorus, respectively, some agglomerations of  $\text{H}_3\text{BO}_3$  were observed.

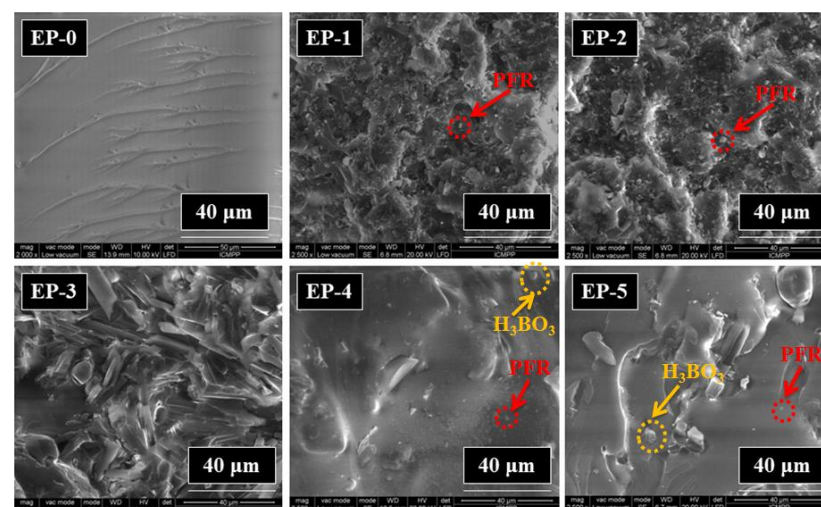


Figure 6. SEM micrographs of epoxy composite surface.

### 3.3. Thermal Characterization of Epoxy Composites

The thermal stability of epoxy composites was evaluated by TGA analysis. The main parameters  $T_{onset}$  (the temperature at which the thermal degradation starts),  $T_{max}$  (the temperature at which the mass loss rate is the highest), and char yield (mass residue remaining after thermal degradation at 800 °C) are summarized in Table 2. Figure 7 shows the TG and DTG curves of epoxy composites. The samples exhibited two steps of weight loss. The first step, in the temperature range of 100–250 °C, was due to the thermal decomposition of PFR, first thermal dehydration of  $H_3BO_3$ , and second thermal dehydration of the latter [29,44]. The second step of weight loss appeared in the temperature range of 300–550 °C, due to the thermal decomposition of polymer matrix [43]. The  $T_{onset}$  of the second step of thermal decomposition was in the interval 295–342 °C. The introduction of PFR and  $H_3BO_3$  slightly decreased  $T_{onset}$  of the samples due to the lower thermal stability of PFR and thermal dehydration process of  $H_3BO_3$ .

**Table 2.** Thermal properties of epoxy composites.

Sample	$T_g$ <sup>1</sup> (°C)	$T_{onset}$ <sup>2</sup> (°C)	$T_{max}$ <sup>3</sup> (°C)	Char Yield <sup>4</sup> (wt%)
EP-0	55.6	342	373	14.57
EP-1	53.0	307	344	14.04
EP-2	52.5	303	336	12.91
EP-3	56.0	295	330	17.95
EP-4	71.0	323	373	21.51
EP-5	64.5	308	357	25.60

<sup>1</sup> Glass transition temperature; <sup>2</sup> Temperature at which the thermal degradation starts, in the second step of weight loss; <sup>3</sup> Temperature at which the mass loss rate is the highest in the second step of weight loss; <sup>4</sup> Char yield after thermal degradation at 800 °C.

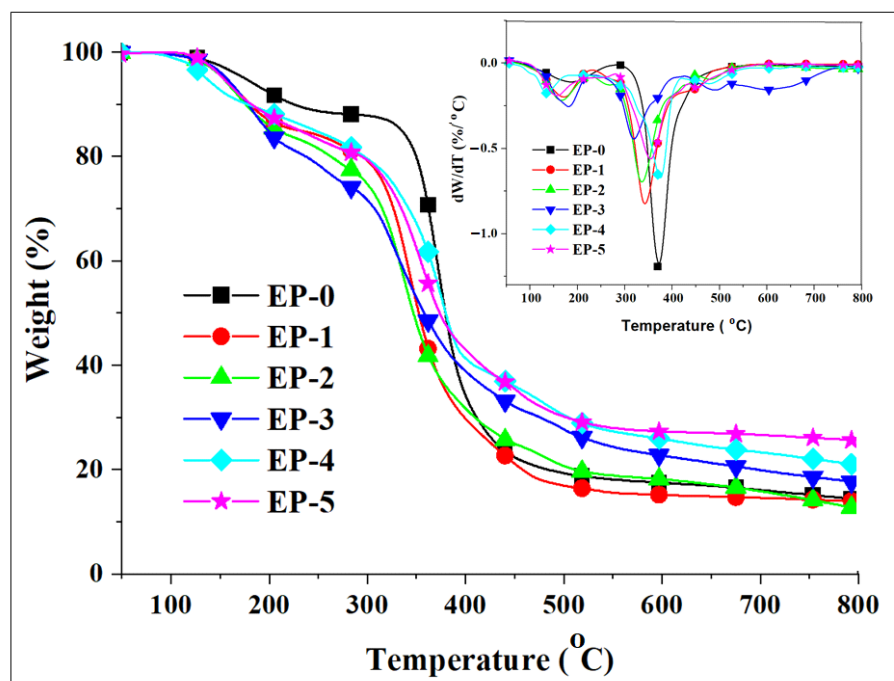


**Figure 7.** TG and DTG curves (inset) of epoxy composites.

The maximum weight loss temperature in the second step of decomposition was in the interval 330–370 °C. This temperature decreased slightly as the PFR content increased. As can be seen from Figure 7 inset, the neat epoxy thermoset showed the highest weight loss rate (WLR) of 1.161 %/°C at 375 °C. The introduction of phosphorus-containing PFR decreased WLR; for example, for EP-3 containing 4 wt% phosphorus, the WLR was

0.435 %/°C. Moreover, EP-4 and EP-5 containing 2 wt% boron and 1.5 or 2 wt% phosphorus exhibited lower WLR values (0.655 and 0.516 %/°C, respectively).

The char yield values at 800 °C were in the interval 12.9–25.6 wt%. The chars of the samples were relatively stable in the temperature interval of 500–800 °C. The lowest values of the char yield were obtained for the EP-0, EP-1 and EP-2 having lower phosphorus content. An increase in the char yield value was observed for the EP-3 containing 4 wt% phosphorus. The highest values of the char yield were obtained for EP-4 and EP-5 containing 2 wt% boron and 1.5 and 2 wt% phosphorus, respectively. This could be attributed to a synergistic effect of PFR containing phosphorus and H<sub>3</sub>BO<sub>3</sub> in increasing the char yield values [28]. It is advantageous to have a higher char yield value because in this case a smaller amount of polymeric material is decomposed, thus resulting in a smaller volume of combustible gases that can cause a fire. This effect has been also observed by other researchers when H<sub>3</sub>BO<sub>3</sub> was used together with a phosphorus-containing compound to improve the flame-resistant characteristics of epoxy resins [38].

The glass transition temperature ( $T_g$ ) of the samples was in the interval 52.5–71.0 °C (Table 2, Figure 8). An increase in  $T_g$  appeared for the samples containing both H<sub>3</sub>BO<sub>3</sub> and PFR (EP-4 and EP-5), probably because of increased co-interaction between H<sub>3</sub>BO<sub>3</sub> and PFR with the polymer matrix that resulted in an increase in the rigidity of the macromolecular chains thus increasing the  $T_g$  values.

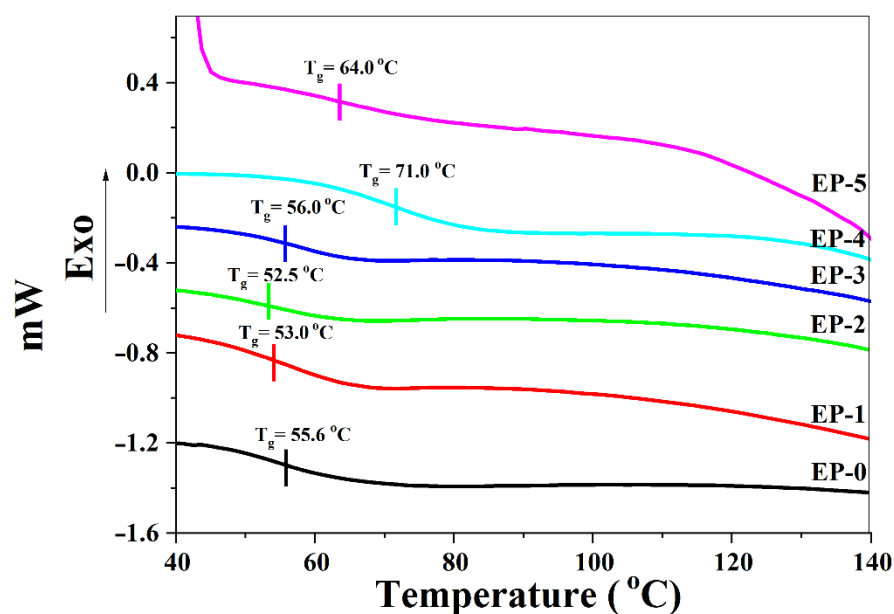
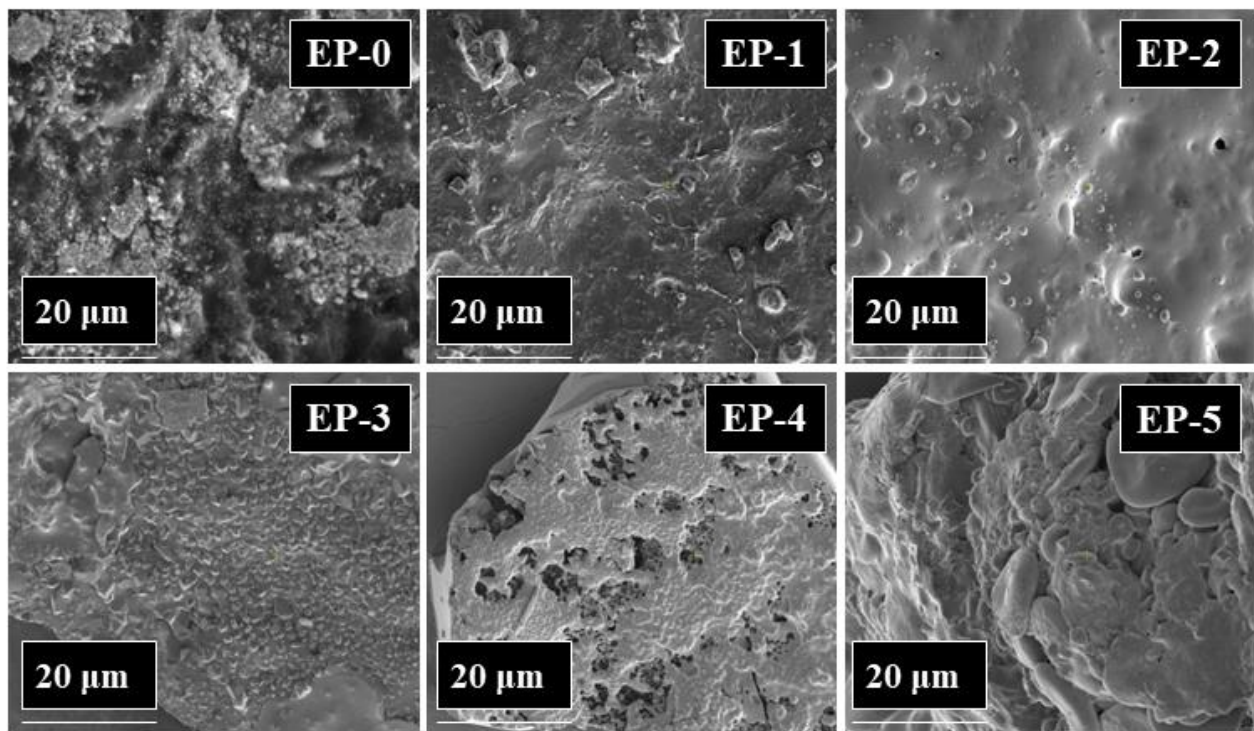
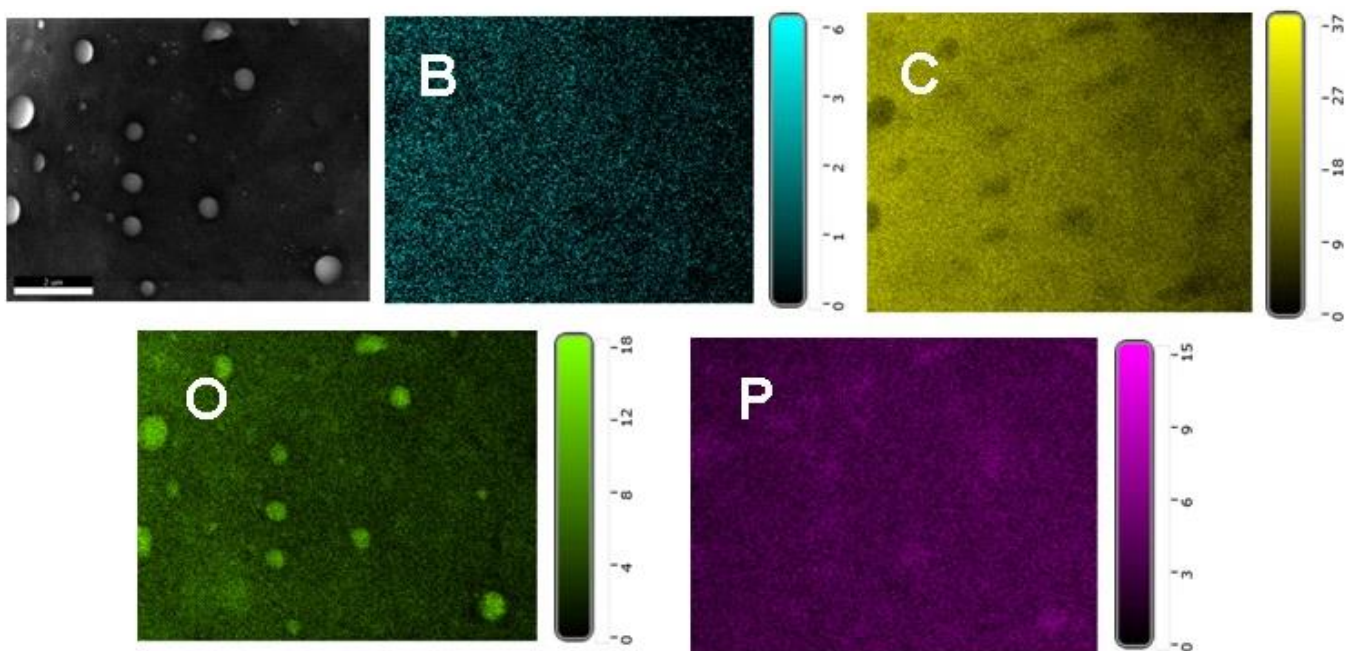


Figure 8. DSC curves of epoxy composites.

The char residue formed during a fire behaves as a protective layer against the transport of heat and combustible gases. The effectiveness of this protection depends on the quantity and morphology of the char. The SEM images of pyrolyzed composite chars obtained by heating the samples up to 800 °C with the heating rate of 10 °C/min in nitrogen atmosphere are shown in Figure 9. As can be seen from Figure 9, the EP-0 char is porous, having many holes, while the chars of samples containing phosphorus EP-1, EP-2 and EP-3 were more compact and denser. Thus, PFR, a compound derived from DOPO, improved the morphology of the chars. The chars of EP-4 and EP-5 were also compact and dense when compared with those of EP-0. A mapping technique was used to investigate the atom distribution on the char surface. From Figure 10, which presents the EDX mapping of EP-5 char, it can be observed that the phosphorus and boron atoms have been present and are uniformly distributed on the char residue surface.



**Figure 9.** SEM micrographs of epoxy composites heated up to 800 °C, with the heating rate of 10 °C/min, under nitrogen atmosphere.



**Figure 10.** EDX mapping of EP-5 char.

Figure 11 presents the FTIR spectra of EP-5, and EP-5 heated up to 520 °C with the heating rate of 10 °C/min in a nitrogen atmosphere. In the FTIR spectrum of thermally treated EP-5, a decrease in the intensity of characteristic peaks for aliphatic groups at 2968, 2922 and 2868  $\text{cm}^{-1}$  can be observed. A strong absorption band characteristic for the presence of aromatic systems appeared at 1630  $\text{cm}^{-1}$ . The absorption bands at 1440 and 754  $\text{cm}^{-1}$  were attributed to P-C and B-O-B bonds in char residue. As was also evidenced by EDX mapping of EP-5 char, it can be concluded that at high temperature the

decomposition of EP-5 took place with the degradation of aliphatic groups of epoxy resin and an increase in phosphorus and boron content in the char residue.

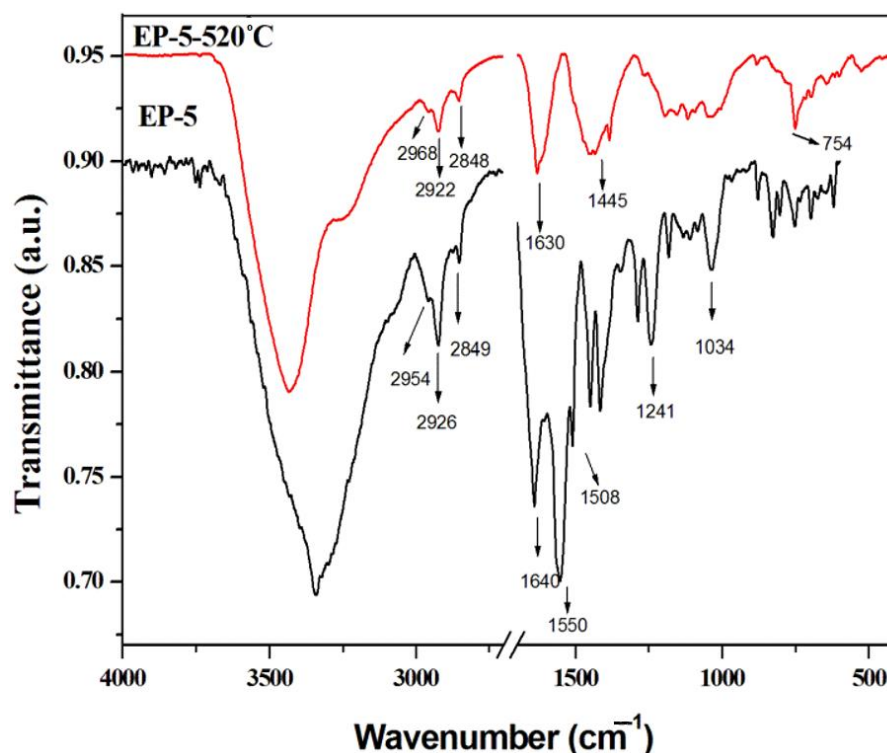


**Figure 11.** FTIR spectra of EP-5 and EP-5 heated up to 520 °C.

### 3.4. Microscale Combustion Calorimetry (MCC) Tests

Microscale combustion calorimetry (MCC) tests were used to evaluate the flammability of the samples. MCC is an important method for evaluating the combustion behavior of polymer materials [45,46]. The main thermal combustion parameters such as char yield (CY), total heat release, heat release capacity (HRC), the peak of heat release rate (PHRR), the temperature of the heat release peak, and the time to obtain the heat release peak are presented in Table 3. Figure 12a,b presents the dependence of the heat release rate (HRR) with the temperature and time, respectively. As can be seen from Figure 12a, the HRR of EP-0 strongly increased in the interval 340–500 °C. The thermo-oxidative degradation process occurs in several stages with a heat release in each of them. The greatest amount of heat is produced in different stages, dependent of the sample composition. EP-0 exhibited the maximum value of PHRR (383 W/g). A decrease in this parameter appeared by introducing PFR containing phosphorus. Thus, EP-1, EP-2 and EP-3 containing 2, 3 or 4 wt% phosphorus had PHRR values of 295, 216 and 158 W/g, respectively. Moreover, the incorporation of H<sub>3</sub>BO<sub>3</sub> substantially decreased the PHRR values. Thus EP-5, containing 2 wt% phosphorus and 2 wt% boron, revealed a PHRR value of 172 W/g (Table 3). It can be noticed that a decrease in the time to obtain the heat release peak is caused by increasing the PFR content and the presence of H<sub>3</sub>BO<sub>3</sub>.

**Table 3.** Data obtained by MCC analysis for epoxy composites.

Sample	Char yield (wt%)	THR <sup>1</sup> (kJ/g)	HRC <sup>2</sup> (J/g*K)	PHRR <sup>3</sup> (W/g)	T <sub>PHRR</sub> <sup>4</sup> (°C)	Time <sup>5</sup> (s)
EP-0	6.27	26.5	513	383	387	249
EP-1	7.04	24.2	344	295	341	219
EP-2	7.12	23.2	282	215	337	195
EP-3	5.94	21.9	287	158	354	220
EP-4	18.17	18.9	282	231	410	212
EP-5	20.08	20.4	213	172	365	228

<sup>1</sup> Total heat release; <sup>2</sup> Heat release capacity; <sup>3</sup> Heat release peak; <sup>4</sup> Temperature of heat release peak; <sup>5</sup> The time to attain the heat release peak.

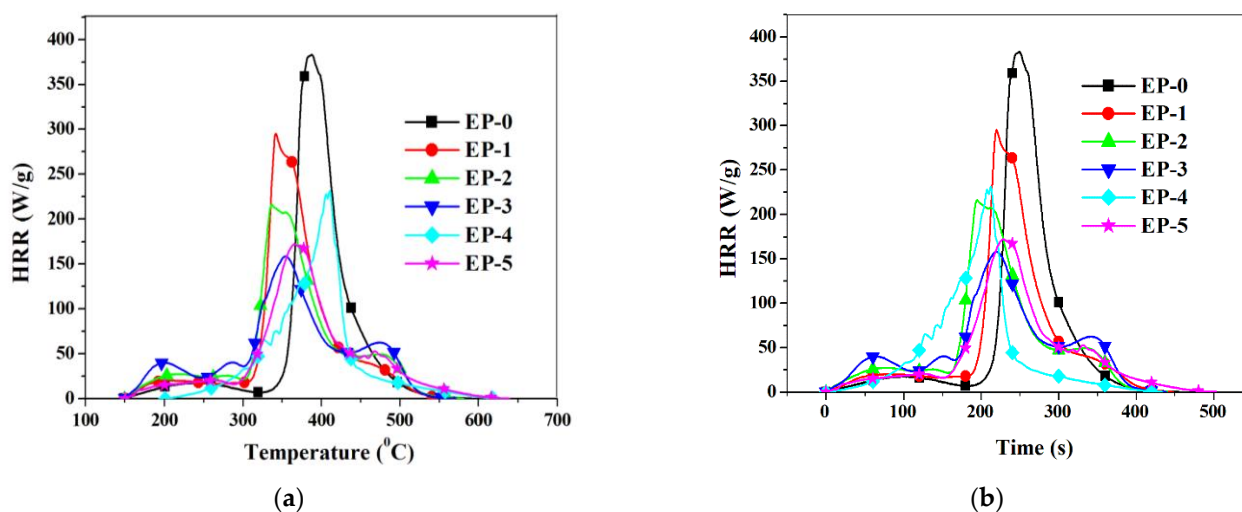


**Figure 12.** (a) Heat release rates versus temperature for epoxy composites; (b) Heat release rates versus time for epoxy composites.

EP-0 exhibited the highest value of THR (26.5 kJ/g). A decrease in THR values can be observed in the case of epoxy thermosets containing phosphorus EP-1, EP-2 and EP-3. The lowest value of THR was obtained for EP-3 containing 4 wt% phosphorus (21.9 kJ/mol). The incorporation of H<sub>3</sub>BO<sub>3</sub> together with compound PFR, in the case of EP-4 and EP-5, substantially decreased THR values, the lowest values being obtained for EP-4 containing 1.5 wt% P and 2 wt% boron (THR = 18.9 kJ/g).

The HRC can be calculated from the MCC test and can be used to classify the flammability of materials, where a low HRC value indicates low flammability of the sample. The HRC of EP-0 was 513 J/(g·K). A substantial decrease in HRC was obtained by incorporating PFR. Thus, sample EP-3 containing 4 wt% phosphorus had an HRC value of 287 J/(g·K). The lowest value of HRC was obtained in the case of EP-5 containing 2 wt% phosphorus and 2 wt% boron (HRC = 213 J/(g·K); this value is lower than those of the EP-2 and EP-3 containing 3 and 4 wt% phosphorus, respectively. It can be concluded that simultaneous incorporation of PFR and H<sub>3</sub>BO<sub>3</sub> improved considerably the flame resistance of epoxy thermosets.

The char yield (CY) resulting from MCC analysis was in the interval 5.94–20.08 wt%. As it can be seen from Table 3, in the case of EP-1, EP-2 and EP-3, CY values did not increase by increasing the phosphorus content. A substantial increase in CY values were noticed for the samples containing both phosphorus and boron elements. Thus, the neat EP-0 exhibited a CY value of 6.27 wt%, while EP-4 and EP-5 had CY values of 18.17 and 20.08 wt%, respectively. The increase in the residue in the case of EP-4 and EP-5 compared with the neat epoxy thermoset EP-0 indicates the formation of a lower amount of combustible gaseous products. Moreover, as was shown in SEM analyses of EP-4 and EP-5 pyrolysis, the char residues exhibited a compact and dense morphology which explains the much

lower values for HRC, THR and PHRR determined by MCC tests on compared with those of the neat epoxy thermoset.

#### 4. Conclusions

New environmentally friendly flame-resistant epoxy composites were prepared by the incorporation of PFR and  $H_3BO_3$  into the epoxy resin. Pyrolysis of epoxy composites containing phosphorus and boron atoms produced a char residue with a compact structure that could act as a barrier to inhibit gaseous products and to insulate the polymer from heat and air. The higher char yield of the samples containing  $H_3BO_3$  was beneficial for improving the flame retardance. The SEM micrograph of EP-4 and EP-5 char residues showed the presence of phosphorus and boron atoms distributed relatively uniformly on the char surface. The MCC analyzer revealed that the introduction of 2 wt% boron and 2 wt% phosphorus considerably decreased the flammability of epoxy thermoset. For this sample the THR and HRC greatly decreased, whereas the residue amount increased considerably. In comparison to pure EP-0, the MCC results displayed that the PHRR, THR and HRC values were decreased by 55.03, 22.93 and 58.365%, respectively. In conclusion, the flame resistance of epoxy resin was significantly improved by simultaneous incorporation of a DOPO derivative and  $H_3BO_3$ . It was demonstrated that these two components did possess a positive role in the condensed phase. In respect of environmental protection, the use of PFR and  $H_3BO_3$  as flame retardants for epoxy resins is promising.

**Author Contributions:** Conceptualization, C.H. and T.V.-B.; methodology, C.H., T.V.-B., I.A., I.-E.S., G.L., D.S. and A.-M.M.; validation, C.H., T.V.-B., I.A., D.S. and G.L.; formal analysis, C.H., A.-M.M. and T.V.-B.; investigation, I.-E.S., G.L., D.S. and A.-M.M.; resources, C.H. and T.V.-B.; writing—original draft preparation, C.H., I.A., G.L. and T.V.-B.; writing—review and editing, T.V.-B. and C.H.; project administration, C.H. and I.A.; funding acquisition, I.A. and G.L. All authors have read and agreed to the published version of the manuscript.

**Funding:** This research received no external funding.

**Data Availability Statement:** The data that support the findings of the current study are listed within the article.

**Acknowledgments:** The author Tăchită Vlad-Bubulac acknowledges the financial support through CNCIS– UEFISCSU, Project Number PN-III-P1-1.1-TE2019-0639 nr. 89/03.09.2020. This work was supported by a grant of the Romanian Minister of Research and Innovation, CCCDI-UEFISCDI, project number PN-III-P1-1. 2-PCCDI-2017-0350/02.03.2018 (Graphene4Life), within PNCDI III.

**Conflicts of Interest:** The authors declare no conflict of interest.

#### References

1. Sukanto, H.; Raharjo, W.W.; Ariawan, D.; Triyono, J.; Kaavesina, M. Epoxy resins thermosetting for mechanical engineering. *Open Eng.* **2021**, *11*, 797–814. [[CrossRef](#)]
2. Capricho, J.C.; Fox, B.; Hameed, N. Multifunctionality in Epoxy Resins. *Polym. Rev.* **2020**, *60*, 1–41. [[CrossRef](#)]
3. Jin, F.-L.; Li, X.; Park, S.-J. Synthesis and application of epoxy resins: A review. *J. Ind. Eng. Chem.* **2015**, *29*, 1–11. [[CrossRef](#)]
4. Kurita, H.; Ishigami, R.; Wu, C.; Narita, F. Mechanical properties of mechanically-defibrated cellulose nanofiber reinforced epoxy resin matrix composites. *J. Compos. Mater.* **2020**, *55*, 455–464. [[CrossRef](#)]
5. Zhao, X.; Lu, S.; Li, W.; Zhang, S.; Li, K.; Nawaz, K.; Wang, P.; Yang, G.; Ragauskas, A.; Ozcan, S.; et al. Epoxy as Filler or Matrix for Polymer Composites. In *Epoxy-Based Composites*; Chelladurai, S.J.S., Arthanari, R., Meera, M.M.R., Eds.; IntechOpen: London, UK, 2022. [[CrossRef](#)]
6. Fattahi, A.M.; Safaei, B.; Qin, Z.; Chu, F. Experimental studies on elastic properties of high density polyethylene-multi walled carbon nanotube nanocomposites. *Steel Compos. Struct.* **2021**, *38*, 177–187. [[CrossRef](#)]
7. Bourbigot, S.; Duquesne, S. Fire retardant polymers: Recent developments and opportunities. *J. Mater. Chem.* **2007**, *17*, 2283–2300. [[CrossRef](#)]
8. Carja, I.-D.; Serbezeanu, D.; Vlad-Bubulac, T.; Hamciuc, C.; Coroaba, A.; Lisa, G.; López, C.G.; Soriano, M.F.; Pérez, V.F.; Romero Sánchez, M.D. A straightforward, eco-friendly and cost-effective approach towards flame retardant epoxy resins. *J. Mater. Chem. A* **2014**, *2*, 16230–16241. [[CrossRef](#)]
9. Chow, W.S.; Chang, L.N.; Jaafar, M. Flame retardant epoxy hybrid composite laminates prepared by vacuum-assisted resin infusion technique. *J. Compos. Mater.* **2014**, *49*, 1471–1481. [[CrossRef](#)]

10. Weil, E.D.; Levchik, S. A Review of Current Flame Retardant Systems for Epoxy Resins. *J. Fire Sci.* **2004**, *22*, 25–40. [[CrossRef](#)]
11. Shaw, S.D.; Blum, A.; Weber, R.; Kannan, K.; Rich, D.; Lucas, D.; Koshland, C.P.; Dobraca, D.; Hanson, S.; Birnbaum, L.S. Halogenated flame retardants: Do the fire safety benefits justify the risks? *Rev. Environ. Health* **2010**, *25*, 261–305. [[CrossRef](#)]
12. You, G.; Cheng, Z.; Peng, H.; He, H. Synthesis and performance of a novel nitrogen-containing cyclic phosphate for intumescent flame retardant and its application in epoxy resin. *J. Appl. Polym. Sci.* **2015**, *132*, 41859. [[CrossRef](#)]
13. Yuan, Y.; Shi, Y.; Yu, B.; Zhan, J.; Zhang, Y.; Song, L.; Ma, C.; Hu, Y. Facile synthesis of aluminum branched oligo(phenylphosphonate) submicro-particles with enhanced flame retardance and smoke toxicity suppression for epoxy resin composites. *J. Hazard. Mater.* **2020**, *381*, 121233. [[CrossRef](#)] [[PubMed](#)]
14. Rakotomalala, M.; Wagner, S.; Döring, M. Recent Developments in Halogen Free Flame Retardants for Epoxy Resins for Electrical and Electronic Applications. *Materials* **2010**, *3*, 4300–4327. [[CrossRef](#)] [[PubMed](#)]
15. Liu, Q.; Wang, D.; Li, Z.; Li, Z.; Peng, X.; Liu, C.; Zhang, Y.; Zheng, P. Recent Developments in the Flame-Retardant System of Epoxy Resin. *Materials* **2020**, *13*, 2145. [[CrossRef](#)]
16. Hamciuc, C.; Serbezeanu, D.; Carja, I.-D.; Vlad-Bubulac, T.; Musteata, V.-E.; Forrat Pérez, V.; Guillem López, C.; López Buendia, A.M. Effect of DOPO units and of polydimethylsiloxane segments on the properties of epoxy resins. *J. Mater. Sci.* **2013**, *48*, 8520–8529. [[CrossRef](#)]
17. Movahedifar, E.; Vahabi, H.; Saeb, M.R.; Thomas, S. Flame Retardant Epoxy Composites on the Road of Innovation: An Analysis with Flame Retardancy Index for Future Development. *Molecules* **2019**, *24*, 3964. [[CrossRef](#)]
18. Huo, S.; Song, P.; Yu, B.; Ran, S.; Chevali, V.S.; Liu, L.; Fang, Z.; Wang, H. Phosphorus-containing flame retardant epoxy thermosets: Recent advances and future perspectives. *Prog. Polym. Sci.* **2021**, *114*, 101366. [[CrossRef](#)]
19. Xiong, Y.-Q.; Zhang, X.-Y.; Liu, J.; Li, M.-M.; Guo, F.; Xia, X.-N.; Xu, W.-J. Synthesis of novel phosphorus-containing epoxy hardeners and thermal stability and flame-retardant properties of cured products. *J. Appl. Polym. Sci.* **2012**, *125*, 1219–1225. [[CrossRef](#)]
20. Hamciuc, C.; Vlad-Bubulac, T.; Serbezeanu, D.; Carja, I.-D.; Hamciuc, E.; Lisa, G.; Pérez, V.F. Environmentally friendly fire-resistant epoxy resins based on a new oligophosphonate with high flame retardant efficiency. *RSC Adv.* **2016**, *6*, 22764–22776. [[CrossRef](#)]
21. Hamciuc, C.; Vlad-Bubulac, T.; Serbezeanu, D.; Carja, I.-D.; Hamciuc, E.; Anghel, I.; Enciu, V.; Şofran, I.-E.; Lisa, G. New fire-resistant epoxy thermosets: Nonisothermal kinetic study and flammability behavior. *J. Polym. Eng.* **2020**, *40*, 21–29. [[CrossRef](#)]
22. Hamciuc, C.; Vlad-Bubulac, T.; Petreus, O.; Lisa, G. Kinetics of thermal degradation in non-isothermal conditions of some phosphorus-containing polyesters and polyesterimides. *Eur. Polym. J.* **2007**, *43*, 980–988. [[CrossRef](#)]
23. Bifulco, A.; Varganici, C.D.; Rosu, L.; Mustata, F.; Rosu, D.; Gaan, S. Recent advances in flame retardant epoxy systems containing non-reactive DOPO based phosphorus additives. *Polym. Degrad. Stab.* **2022**, *200*, 109962. [[CrossRef](#)]
24. Varganici, C.D.; Rosu, L.; Lehner, S.; Hamciuc, C.; Jovic, M.; Rosu, D.; Mustata, F.; Gaan, S. Semi-interpenetrating networks based on epoxy resin and oligophosphonate: Comparative effect of three hardeners on the thermal and fire properties. *Mater. Des.* **2021**, *212*, 110237. [[CrossRef](#)]
25. Huang, W.; Wang, K.; Tu, C.; Xu, X.; Tian, Q.; Ma, C.; Fu, Q.; Yan, W. Synergistic Effects of DOPO-Based Derivative and Organo-Montmorillonite on Flame Retardancy, Thermal Stability and Mechanical Properties of Polypropylene. *Polymers* **2022**, *14*, 2372. [[CrossRef](#)] [[PubMed](#)]
26. Sai, T.; Ran, S.; Guo, Z.; Yan, H.; Zhang, Y.; Wang, H.; Song, P.; Fang, Z. Transparent, highly thermostable and flame retardant polycarbonate enabled by rod-like phosphorous-containing metal complex aggregates. *Chem. Eng. J.* **2021**, *409*, 128223. [[CrossRef](#)]
27. Benin, V.; Gardelle, B.; Morgan, A.B. Heat release of polyurethanes containing potential flame retardants based on boron and phosphorus chemistries. *Polym. Degrad. Stab.* **2014**, *106*, 108–121. [[CrossRef](#)]
28. Dogan, M.; Dogan, S.D.; Savas, L.A.; Ozcelik, G.; Tayfun, U. Flame retardant effect of boron compounds in polymeric materials. *Compos. Part B Eng.* **2021**, *222*, 109088. [[CrossRef](#)]
29. Nazarenko, O.B.; Bukhareva, P.B.; Melnikova, T.V.; Visakh, P.M. Effect of Boric Acid on Volatile Products of Thermooxidative Degradation of Epoxy Polymers. *J. Phys. Conf. Ser.* **2016**, *671*, 012041. [[CrossRef](#)]
30. Lu, S.-Y.; Hamerton, I. Recent developments in the chemistry of halogen-free flame retardant polymers. *Prog. Polym. Sci.* **2002**, *27*, 1661–1712. [[CrossRef](#)]
31. Wang, L.; He, X.; Wilkie, C.A. The Utility of Nanocomposites in Fire Retardancy. *Materials* **2010**, *3*, 4580–4606. [[CrossRef](#)]
32. Nagieb, Z.A.; Nassar, M.A.; El-Meligy, M.G. Effect of Addition of Boric Acid and Borax on Fire-Retardant and Mechanical Properties of Urea Formaldehyde Saw Dust Composites. *Int. J. Carbohydr. Chem.* **2011**, *2011*, 146763. [[CrossRef](#)]
33. Murat Unlu, S.; Tayfun, U.; Yildirim, B.; Dogan, M. Effect of boron compounds on fire protection properties of epoxy based intumescent coating. *Fire Mater.* **2017**, *41*, 17–28. [[CrossRef](#)]
34. Huber, C.; Jahromy, S.S.; Birkelbach, F.; Weber, J.; Jordan, C.; Schreiner, M.; Harasek, M.; Winter, F. The multistep decomposition of boric acid. *Energy Sci. Eng.* **2020**, *8*, 1650–1666. [[CrossRef](#)]
35. Nazarenko, O.B.; Amelkovich, Y.A.; Bannov, A.G.; Berdyugina, I.S.; Maniyan, V.P. Thermal Stability and Flammability of Epoxy Composites Filled with Multi-Walled Carbon Nanotubes, Boric Acid, and Sodium Bicarbonate. *Polymers* **2021**, *13*, 638. [[CrossRef](#)] [[PubMed](#)]
36. Visakh, P.M.; Nazarenko, O.B.; Amelkovich, Y.A.; Melnikova, T.V. Effect of zeolite and boric acid on epoxy-based composites. *Polym. Adv. Technol.* **2016**, *27*, 1098–1101. [[CrossRef](#)]

37. Unlu, S.M.; Dogan, S.D.; Dogan, M. Comparative study of boron compounds and aluminum trihydroxide as flame retardant additives in epoxy resin. *Polym. Adv. Technol.* **2014**, *25*, 769–776. [[CrossRef](#)]
38. Chen, Y.; Duan, H.; Ji, S.; Ma, H. Novel phosphorus/nitrogen/boron-containing carboxylic acid as co-curing agent for fire safety of epoxy resin with enhanced mechanical properties. *J. Hazard. Mater.* **2021**, *402*, 123769. [[CrossRef](#)]
39. Yang, S.; Zhang, Q.; Hu, Y. Synthesis of a novel flame retardant containing phosphorus, nitrogen and boron and its application in flame-retardant epoxy resin. *Polym. Degrad. Stab.* **2016**, *133*, 358–366. [[CrossRef](#)]
40. Wang, X.-Z. Crystal structure of 6-(hydroxy(phenyl)methyl)-6H-dibenzo[c,e][1,2]-oxaphosphinine 6-oxide, C<sub>19</sub>H<sub>15</sub>O<sub>3</sub>P. *Z. Krist. New Cryst. Struct.* **2014**, *229*, 227–228. [[CrossRef](#)]
41. ASTM D7309-21b; Standard Test Method for Determining Flammability Characteristics of Plastics and Other Solid Materials Using Microscale Combustion Calorimetry. ASTM International: West Conshohocken, PA, USA, 2007.
42. Przystas, A.; Jovic, M.; Salmeia, K.A.; Rentsch, D.; Ferry, L.; Misprouve, H.; Perler, H.; Gaan, S. Some Key Factors Influencing the Flame Retardancy of EDA-DOPO Containing Flexible Polyurethane Foams. *Polymers* **2018**, *10*, 1115. [[CrossRef](#)]
43. Liu, X.; Salmeia, K.A.; Rentsch, D.; Hao, J.; Gaan, S. Thermal decomposition and flammability of rigid PU foams containing some DOPO derivatives and other phosphorus compounds. *J. Anal. Appl. Pyrolysis* **2017**, *124*, 219–229. [[CrossRef](#)]
44. Sevim, F.; Demir, F.; Bilen, M.; Okur, H. Kinetic analysis of thermal decomposition of boric acid from thermogravimetric data. *Korean J. Chem. Eng.* **2006**, *23*, 736–740. [[CrossRef](#)]
45. Wilkie, C.A.; Chigwada, G.; Gilman, S.J.W.; Lyon, R.E. High-throughput techniques for the evaluation of fire retardancy. *J. Mater. Chem.* **2006**, *16*, 2023–2030. [[CrossRef](#)]
46. Lyon, R.E.; Walters, R.N. Pyrolysis combustion flow calorimetry. *J. Anal. Appl. Pyrolysis* **2004**, *71*, 27–46. [[CrossRef](#)]